Research Article | Vol. 27, No. 15 | 22 Jul 2019 | OPTICS EXPRESS 20412
Optics EXPRESS

Achieving the laser intensity of 5.5×10^{22} W/cm^2 with a wavefront-corrected multi-PW laser

JIN WOO YOON,[1,2] CHEONHA JEON,[1] JUNGHOON SHIN,[1] SEONG KU LEE,[1,2] HWANG WOON LEE,[1] IL WOO CHOI,[1,2] HYUNG TAEK KIM,[1,2] JAE HEE SUNG[1,2,4] AND CHANG HEE NAM,[1,3,5]

[1] *Center for Relativistic Laser Science, Institute for Basic Science, 123 Cheomdangwagi-ro, Buk-gu, Gwangju, 61005, South Korea*
[2] *Advanced Photonics Research Institute, Gwangju Institute of Science and Technology, 123 Cheomdangwagi-ro, Buk-gu, Gwangju, 61005, South Korea*
[3] *Dept. of Physics and Photon Science, Gwangju Institute of Science and Technology, 123 Cheomdangwagi-ro, Buk-gu, Gwangju, 61005, South Korea*
[4] *sungjh@gist.ac.kr*
[5] *chnam@gist.ac.kr*

Abstract: The generation of ultrahigh intensity laser pulses was investigated by tightly focusing a wavefront-corrected multi-petawatt Ti:sapphire laser. For the wavefront correction of the PW laser, two stages of deformable mirrors were employed. The multi-PW laser beam was tightly focused by an $f/1.6$ off-axis parabolic mirror and the focal spot profile was measured. After the wavefront correction, the Strehl ratio was about 0.4, and the spot size in full width at half maximum was 1.5×1.8 μm^2, close to the diffraction-limited value. The measured peak intensity was 5.5×10^{22} W/cm^2, achieving the highest laser intensity ever reached.

1. Introduction

Since the invention of laser in 1960, the peak power of lasers has increased rapidly with the development of the mode-locking and the chirped-pulse amplification techniques [1]. A number of petawatt lasers are currently in operation around the world [2–9], and they have become essential research tools for investigating the interactions of strong light and matter. In this regard, the most important laser parameter is the laser intensity, which determines the regime of the interaction, e.g. linear, weakly nonlinear, strongly nonlinear, relativistic, and even quantum electrodynamical regimes. Focused intensities of ultrahigh power lasers employed for experiments are mostly in the range of $10^{19} \sim 10^{21}$ W/cm^2. In this intensity range, relativistic optics experiments on electron acceleration, ion acceleration, x-/γ-ray generation, and radiation reaction can be performed [10–12]. For the investigation of extreme phenomena in strong-field quantum electrodynamics, such as nonlinear Compton scattering, light-light interaction, and vacuum birefringence, a laser intensity over 10^{22} W/cm^2 is desired [13–15].

In order to reach a focused intensity over 10^{22} W/cm^2, a laser power has to be boosted and tight focusing has to be performed. For boosting the laser peak power, multi-PW lasers have been developed [8, 9] and are being constructed in a number of institutes around the world [16–19]. In order to obtain the maximum peak intensity from a high power laser the focal spot size has to be minimized. For enhancing the focusability of a laser beam, the wavefront correction using a deformable mirror (DM) system is essential, because a laser beam with wavefront aberration cannot be focused close to the diffraction-limited focal spot (Airy disk) [20–22]. And a focusing optics with a small $f/\#$ is required for reducing the focal spot size, because the Airy disk size is proportional to the $f/\#$ of the focusing optics. The University of Michigan team obtained a peak intensity of 1×10^{22} W/cm^2 with its HERCULES laser in 2004 [23], which was upgraded to 2×10^{22} W/cm^2 by focusing the 300 TW laser beam into 1.3 μm with an $f/1$ off-axis parabolic

#364568 https://doi.org/10.1364/OE.27.020412
Journal © 2019 Received 9 Apr 2019; revised 10 Jun 2019; accepted 12 Jun 2019; published 9 Jul 2019

Optics EXPRESS

mirror (OAP) [24]. In 2017, a peak intensity of 1×10^{22} W/cm^2 was achieved with the J-KAREN-P laser at KPSI (Japan) [25]. Here a 300 TW laser beam was focused to a spot size of 1.3 μm by an $f/1.3$ OAP (f = 350 mm). In 2018, a peak intensity of 2×10^{22} W/cm^2 was achieved with the SULF laser at SIOM (China). A 5.4 PW laser beam was focused by an $f/2.5$ OAP (f = 721 mm) and the wavefront was corrected with double DMs [26]. Through more tight focusing of a multi-PW laser, a higher laser intensity should be achievable.

In this work, the wavefront correction and the tight focusing of a multi-PW laser at Center for Relativistic Laser Science (CoReLS) were investigated to achieve an ultrahigh laser intensity. For the wavefront correction of the PW laser, two stages of DMs were employed. We accurately measured the focal spot of the real PW laser beam focused with an $f/1.6$ OAP. In Sec. 2, the multi-PW laser at CoReLS and the experimental setup are described. In Sec. 3, the wavefront aberrations in the PW laser beamline and their compensation are studied, and the focal spot characterization and the focused laser intensity are presented. In Sec. 4, the conclusion is given.

2. Experimental setup

A 20 fs, 4 PW Ti:sapphire laser operating at 0.1 Hz has been developed at CoReLS [8]. The 4 PW Ti:sapphire laser consists of a femtosecond oscillator, a 1 kHz front-end amplifier, a cross-polarized wave generation stage, a grating pulse stretcher, an OPCPA preamplifier, two power amplifiers, two booster amplifiers, and a grating pulse compressor. Figure 1 shows the layout of the PW laser and the experimental setup. The laser pulse was amplified to 4.5 J in two power amplifiers at 5 Hz repetition rate and amplified to 112 J in two booster amplifiers at 0.1 Hz repetition rate. The laser beam was then up-collimated from 85 mm to 280 mm by the final beam expander in order to avoid the optical damage of the compressor gratings. The final beam expander consisted of spherical mirrors instead of lenses to prevent the chromatic aberration and the increase of the B-integral value. After the final beam expander, the laser pulse was recompressed to 20 fs (FWHM) in the grating pulse compressor, and the Fourier transform-limited pulse duration is 19 fs. The pulse compressor was comprised of four high quality gratings, manufactured by Lawrence Livermore National Laboratory, with a surface roughness about 40 nm (rms) and a holographic error less than $\lambda/10$. The pulse duration was measured with a SPIDER right after the pulse compressor. And the measurement was done in air using a 3 mm diameter sample beam, which passed through a 2 mm thick fused silica window. The dispersion of the window and air was subtracted by post-processing. To check the influence of the spatio-temporal coupling on the pulse duration, we measured pulse duration with full aperture beam. The full beam was down-collimated with a spherical focusing mirror with f = 12, 000 mm and an OAP with f = 150 mm, and then the pulse duration was measured with the SPIDER. The pulse duration measured with full aperture beam was 20 fs, nearly identical to the one we measured with the sample beam and the shot-to-shot fluctuation of the pulse duration was 0.5 fs (rms). The compressed pulse energy (E_0) was 83 J in the full power operation and the energy stability was 1.5% (rms). The peak power (P_0) of the compressed pulse, 4.0 PW, could be obtained from the relation between the energy and the peak power, $E_0 = P_0 \int p(t)dt$, where $p(t)$ is the normalized instantaneous power.

Two deformable mirrors were employed in the PW laser to fully compensate for its wavefront aberration. In order to correct the wavefront distortion accumulated from the front-end to the final beam expander, a bimorph deformable mirror (DM1, AKA optics) with a diameter of 100 mm and 48 actuators was installed after the final booster amplifier. The DM surface was coated with a broadband dielectric coating in the range from 750 nm to 850 nm. The second deformable mirror (DM2, AKA optics) with a diameter of 300 mm and 127 actuators was installed after the pulse compressor to correct additional aberrations, induced from large aperture optics and focusing optics in the pulse compressor, the beam delivery line and the target area.

For monitoring the wavefront aberration of the PW laser and for controlling the DMs, three

Optics EXPRESS

wavefront sensors were installed in the PW laser, as shown in Fig. 1. The first wavefront sensor (WFS1, Phasics, SID4), located after the second power amplifier, measured the wavefront aberration accumulated from the front-end to the second power amplifier. The second wavefront sensor (WFS2, Phasics, SID4), located right after the final beam expander, measured the total wavefront aberration before the pulse compressor, and the feedback signal from the WFS2 was sent to the DM1 for wavefront correction. The two wavefront sensors, WFS1 and WFS2, were based on the 4-wave shearing interferometer [27]. After being focused with an $f/1.6$ gold-coated OAP (Aperture Optical Sciences) with a 450 mm focal length and a 1 nm surface roughness installed in the target chamber, the laser beam was collimated by an apochromatic objective lens (Mitutoyo, 50×, f = 4.0 mm, N.A. = 0.65), and then divided by a beam splitter, as shown in Fig. 1. Here the spot image of the laser beam focused by the OAP was relay-imaged to a 12-bit CMOS camera (EPIX, SV10M6, 1.67 μm pixel) with a pair of lenses - the objective lens and an achromatic lens (f = 125 mm). The reflected beam from the beam splitter was sent to a Shack-Hartmann wavefront sensor (WFS3, AKA optics, WFS-5-0.100) with an 80×80 microlenslet array, and the deformable mirror surface (DM2) was imaged to WFS3 with a pair of achromatic lenses (f = 200 mm and f = 750 mm). The wavefront aberration at the target area was measured with the WFS3, and the DM2 was controlled by the feedback signal from the WFS3. As a result, an accurate wavefront measurement and a proper wavefront correction could be performed with three wavefront sensors and two DMs, and the resulting laser intensity could be identified through the focal spot measurement. In this work, the laser performance test was carried out in two operational modes - without (100 TW mode) and with (PW mode) pumping two booster amplifiers. In the PW mode, on-target energy was reduced to 63 J due to the pump energy reduction in the booster amplifiers, which corresponded to the peak power of 3.0 PW.

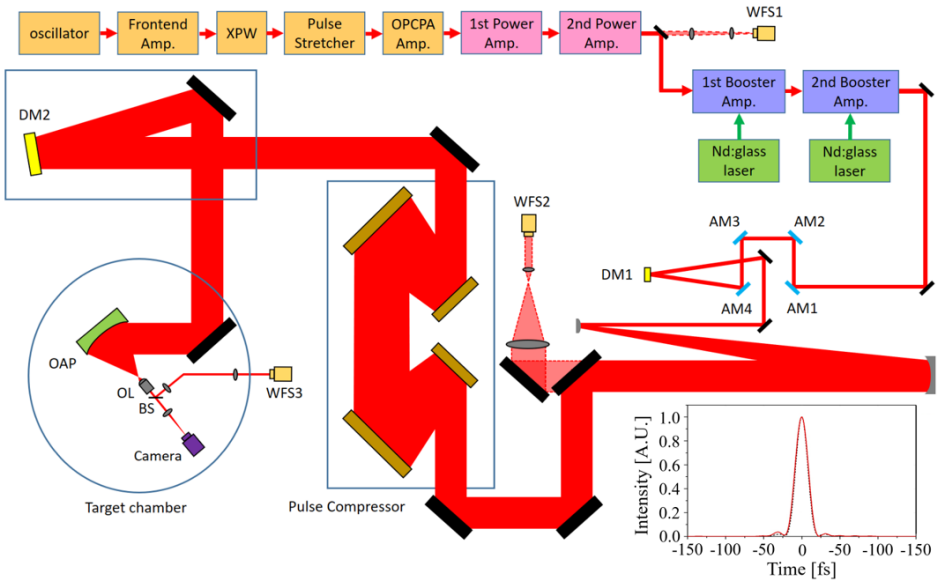

Fig. 1. Layout of the PW laser and the experimental setup. WFS1-3, wavefront sensors; DM1-2, deformable mirrors; AM1-4, attenuation mirrors; OAP, $f/1.6$ off-axis parabolic mirror; OL, objective lens; BS, beam splitter. The inset (bottom right corner) shows the temporal profile measured with a full aperture beam. The measured pulse duration was 20 fs (FWHM).

To avoid nonlinear optical effects and the optical damage of sensors, the laser energy was attenuated with partial reflection mirrors (AM1-4) located after the final booster amplifier. For

Optics EXPRESS

the energy attenuation in the 100 TW mode, four partial reflection mirrors with 1%, 1%, 5% and 100% reflection coating were used. For the energy attenuation of PW beam, four partial reflection mirrors with 1%, 1%, 5% and 1% reflection coating were used. The surface flatness of the attenuation mirrors, measured with a Zygo interferometer, was less than 0.02 μm (rms). The effect of this surface flatness on wavefront distortion was thus negligible. The attenuation mirrors could be easily moved out an in without affecting the main beam alignment by checking the alignment using several beam pointing (near-field and far-field) monitoring optics.

In addition, though thermal loading to compression gratings may be problematic when a high average power laser is injected to the pulse compressor, this kind of thermal load effect was negligible in our PW laser operating at the repetition rate less than 0.1 Hz.

3. Experimental results

3.1. Wavefront aberration of the PW laser

Wavefront aberrations were measured with the wavefront sensors at three positions in the PW laser beamline. The peak-to-valley (PV) value and root-mean-square (RMS) value of the wavefront error at WFS1 were 0.60 μm and 0.14 μm, respectively. In the 100 TW mode (without pumping two booster amplifiers), the PV and RMS values at WFS2 were 0.84 μm and 0.16 μm, respectively. It means that just a little wavefront aberration was induced in the booster amplifiers and the final beam expander. In the 100 TW mode, the PV and RMS values measured at WFS3 were 2.94 μm and 0.45 μm, respectively, and in the PW mode, 3.05 μm and 0.45 μm, respectively. This large PV and large RMS values mean that serious wavefront distortion was induced after the final beam expander. And little difference in measured aberrations between the 100 TW and the PW modes indicates that strong amplification of two booster amplifiers had little influence on the wavefront aberration. The large wavefront aberration was mainly caused by large aperture optical components and the OAP misalignment. This aberration was large enough to deteriorate the focal spot quality, and the wavefront correction using adaptive optics systems was strongly required to achieve the diffraction-limited focusing of the PW laser.

3.2. Wavefront correction and focal spot characterization of the 100 TW beam

The wavefront correction and the focal spot measurement were performed in the 100 TW mode. Figure 2 shows the wavefront maps measured with WFS2 before and after the first DM (DM1) operation in the 100 TW mode. The RMS value of the wavefront error was greatly reduced from 0.16 μm to 0.04 μm after the DM1 operation. In principle, flat wavefront before the pulse compressor is required to avoid spatio-temporal coupling in the pulse compressor [28,29]. In our PW laser, DM1 made the wavefront, before the compressor, flat. Figure 3 shows the wavefront maps and the Zernike coefficients measured with WFS3 in the 100 TW mode before and after the wavefront correction with the second DM (DM2). Before the correction, the RMS value of the wavefront aberration was 0.45 μm. After the correction, the RMS value was dramatically reduced to 0.05 μm. Figure 4 shows the focal spot images measured by the CMOS camera before and after the wavefront correction in the 100 TW mode. The focal spot image after the wavefront correction in Fig. 4(b) shows a quite elliptical shape. When we measured the focal spot with an 800 nm band-pass filter (10 nm bandwidth), there was no elongation, which means that the focal spot distortion in Fig. 4(b) resulted from an angular chirp. For the angular chirp compensation, we adjusted the groove tilt and the horizontal rotation of the third grating in the pulse compressor. After the fine tuning of the grating orientation by 50 μrad, we obtained the almost circular focal spot shown in Fig. 4(c). When the pulse duration was measured again to check the influence of the grating adjustment on temporal duration, the measured pulse duration was nearly the same (20 fs) due to the small amount of the grating adjustment. In Fig. 4(c), the corrected focal spot size in FWHM was measured to be 1.4×1.5 μm^2, very close to the diffraction-limited spot size

of 1.3 μm (FWHM). Furthermore, pulse duration measured with a full aperture beam, 20 fs, was also near Fourier transform-limit (19 fs), which indicates that the spatio-temporal coupling is not significant in our PW laser. In case such focal spot image in Fig. 4(c) were obtained with the full power (P_0 = 4.0 PW), the peak intensity would correspond to 1.1×10^{23} W/cm^2. In the case of the SULF laser with a 5.4 PW peak power at SIOM, a peak intensity of 2×10^{22} W/cm^2 was estimated from the low energy mode operation without pumping the booster amplifiers [26].

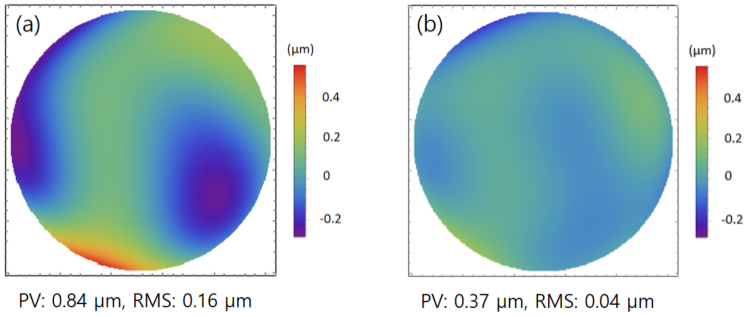

Fig. 2. Wavefront maps measured at WFS2 (a) before and (b) after DM1 operation in the 100 TW mode

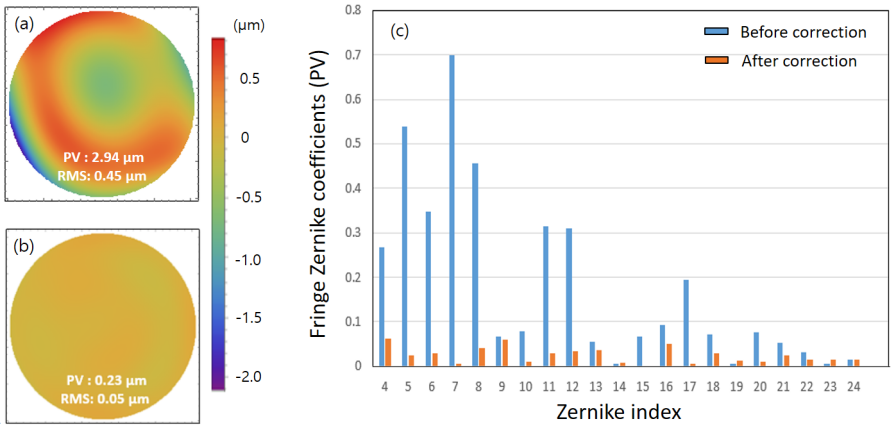

Fig. 3. Wavefront maps measured in the 100 TW mode by WFS3 (a) before the wavefront correction, (b) after the wavefront correction, and (c) the comparison of the Zernike coefficients before and after the wavefront correction.

The Strehl ratio and the encircled energy factor of the measured focal spot were calculated. For the focal spot analysis, background noise was subtracted from the measured focal spot, and then signal was integrated in the range of 30 times the Airy disk. The cross-sectional profiles of the measured focal spot, the ideal focal spot and the point spread function (PSF) are shown in Fig. 5(a). Here the Strehl ratio calculated from the peak intensity of the focal spot was about 0.58. On the contrary, the Strehl ratio calculated from the measured wavefront and the intensity distribution (PSF) was 0.91. This difference was mostly caused by the inaccuracy of wavefront data at the beam edge [25]. As shown in Fig. 5(b), the encircled energy factor of the measured focal spot was 0.33 within FWHM and 0.55 within $1/e^2$.

Optics EXPRESS

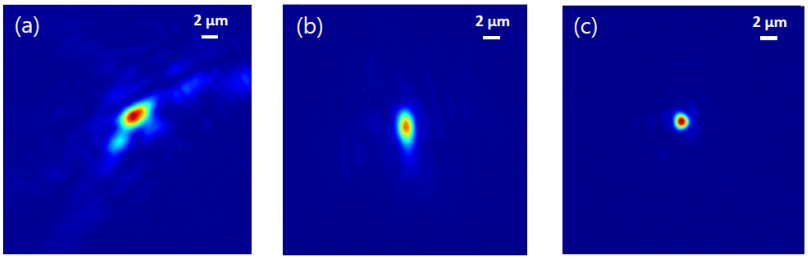

Fig. 4. The focal spot images measured in the 100 TW mode (a) before the wavefront correction, (b) after the wavefront correction, and (c) after the wavefront correction and the fine tuning of the compressor gratings.

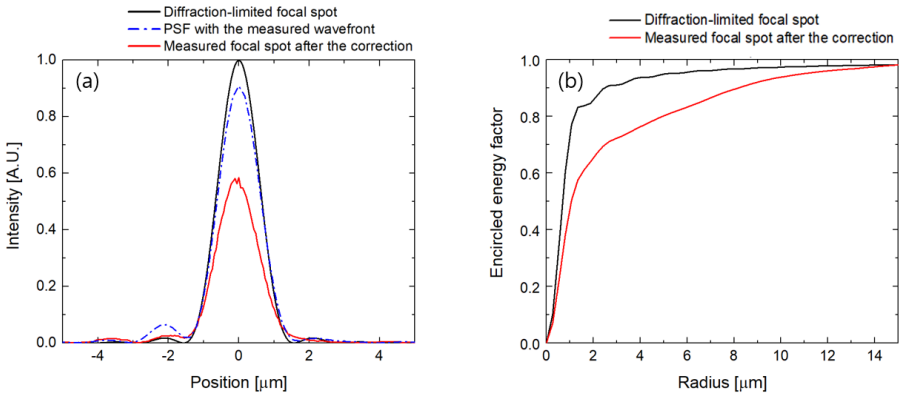

Fig. 5. (a) Cross-sectional profile (horizontal direction) and (b) the encircled energy factor of the focal spot measured after correction in the 100 TW mode, and those of the diffraction-limited focal spot. The PSF calculated with the measured wavefront is also shown in (a).

3.3. *Wavefront correction and focal spot characterization of the PW beam*

As the next step, the focal spot optimization of the PW laser beam through wavefront correction was performed. Figure 6 shows the wavefront maps and the Zernike coefficients measured with WFS3 in the PW mode before and after the wavefront correction with both DMs. After the correction, the RMS wavefront error was dramatically reduced from 0.45 μm to 0.07 μm. Figure 7 shows the focal spot images measured before and after correction. This work was the first measurement of a real PW laser beam with an intensity over 10^{22} W/cm^2, though the focal spot of a PW laser beam was previously measured with a large $f/\#$ focal system [30]. The corrected focal spot size in FWHM was measured to be 1.5×1.8 μm^2. Figure 8(a) shows the cross-sectional profiles of the measured focal spot, the ideal focal spot and the PSF. The Strehl ratio calculated from the peak intensity of the corrected focal spot was about 0.39 and the Strehl ratio calculated from the PSF was 0.84. The encircled energy factor was 0.29 within FWHM and 0.48 within $1/e^2$, as shown in Fig. 8(b). Here the focal spot size in the PW mode was slightly larger than that in the 100 TW mode in Fig. 4(c). This was caused by the different feedback rate of the closed loop adaptive optic system between the 100 TW mode and the PW mode. In the 100 TW mode, the adaptive optics system was operated in a closed loop running at 5 Hz. In other words, the wavefront measurement and the feedback to the deformable mirror were performed at 5 Hz to compensate for the wavefront variation slower than 5 Hz in the 100 TW mode. On the other hand, in the PW mode, the short-term wavefront fluctuation could not be stabilized due to the

Optics EXPRESS

slow feedback rate of 0.1 Hz.

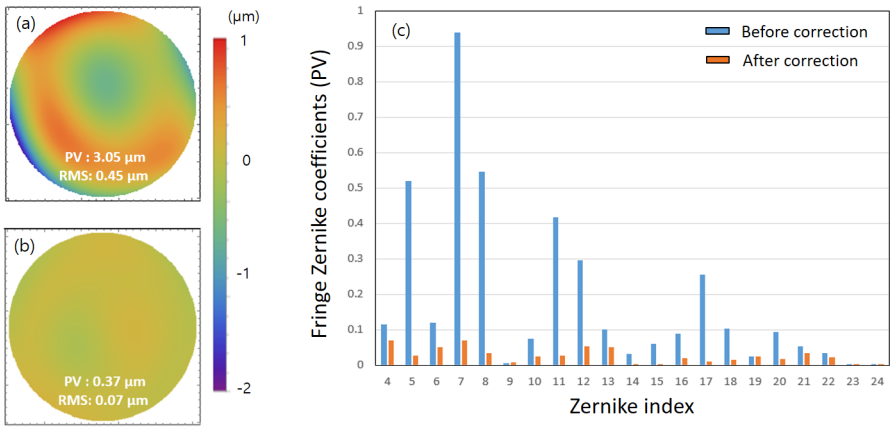

Fig. 6. Wavefront maps measured in the PW mode by WFS3 (a) before the wavefront correction, (b) after the wavefront correction, and (c) the comparison of the Zernike coefficients before and after the wavefront correction.

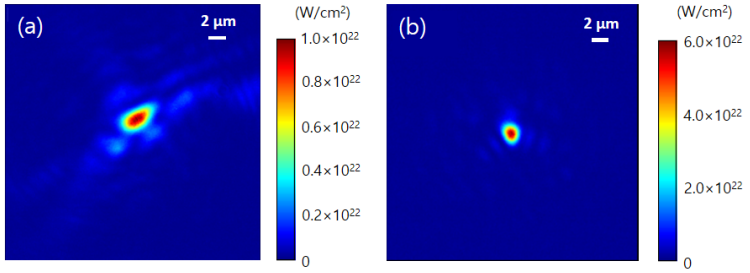

Fig. 7. The focal spot images measured in the PW mode (a) before the wavefront correction and (b) after the wavefront correction

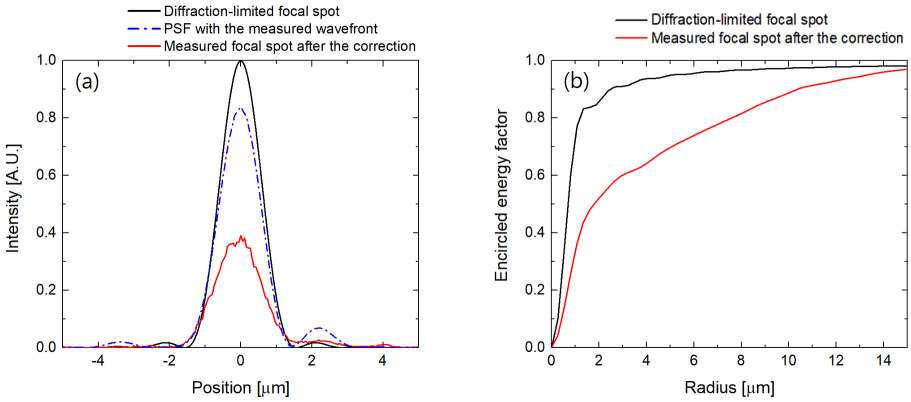

Fig. 8. (a) Cross-sectional profile (horizontal direction) and (b) the encircled energy factor of the focal spot measured after correction in the PW mode, and those of the diffraction-limited focal spot. The PSF calculated with the measured wavefront is also shown in (a).

Optics EXPRESS

The peak laser intensity obtained from the space integral of the intensity distribution ($I(x, y)$) in Fig. 7(b) was 5.5×10^{22} W/cm^2. From the focal spot area measurement of 100 shots, the average value and the fluctuation value (rms) of the peak intensity were 4.9×10^{22} W/cm^2 and 0.35×10^{22} W/cm^2, respectively. The latter was obtained by considering the pulse width fluctuation of 0.5 fs (rms) and the energy fluctuation of 1.5% (rms).

4. Conclusion

In order to achieve ultrahigh peak intensity, a 3.0 PW laser beam was tightly focused by an $f/1.6$ OAP after correcting the wavefront of the PW laser with two stages of DMs located before and after the pulse compressor. After the wavefront correction, the residual RMS wavefront aberration was 0.07 μm and the focal spot size of the 3.0 PW laser beam was 1.5×1.8 μm^2 (FWHM), close to the diffraction-limited focal spot size. The Strehl ratio and the encircled energy factor within $1/e^2$ was 0.39 and 0.48, respectively. When considering fluctuations of the focal spot area, pulse duration and pulse energy, the maximum focused peak intensity obtained was 5.5×10^{22} W/cm^2, while the average value (RMS value) of the focused peak intensity was $4.9(0.35) \times 10^{22}$ W/cm^2, which is the highest peak intensity measured to the best of our knowledge. With the laser pulses of such high intensities, we can explore the novel interaction regime of strong-field quantum electrodynamics, and boost the performance of laser-driven high-energy particle sources.

Funding

Institute for Basic Science (IBS) (IBS-R012-D1); GIST Research Institute (GRI) 2019 grant.

Acknowledgment

We thank Jeong Moon Yang, Yeon Joo Son, Seung Yeon Kim, Han Bum Lim, and Dongyoon Yoo for technical assistance.

References

1. D. Strickland and G. Mourou, "Compression of amplified chirped optical pulses," Opt. Commun. **55**, 447 (1985).
2. C. Danson, D. Hillier, N. Hopps, and D. Neely, "Petawatt class lasers worldwide," High Power Laser Sci. Eng. **3**, e3 (2015).
3. C. Danson, P. Brummitt, R. Clarke, J. Collier, B. Fell, A. Frackiewicz, S. Hancock, S. Hawkes, C. Hernandez-Gomez, P. Holligan, M. Hutchinson, A. Kidd, W. Lester, I. Musgrave, D. Neely, D. Neville, P. Norreys, D. Pepler, C. Reason, W. Shaikh, T. Winstone, R. Wyatt, and B. Wyborn, "Vulcan Petawatt—an ultra-high-intensity interaction facility," Nucl. Fusion **44**, S239 (2004).
4. G. Xu, T. Wang, Z. Li, Y. Dai, Z. Lin, Y. Gu, and J. Zhu, "1 kJ petawatt laser system for SG-II-U program," The Rev. Laser Eng. **36**, 1172 (2008).
5. E. W. Gaul, M. Martinez, J. Blakeney, A. Jochmann, M. Ringuette, D. Hammond, T. Borger, R. Escamilla, S. Douglas, W. Henderson, G. Dyer, A. Erlandson, R. Cross, J. Caird, C. Ebbers, and T. Ditmire, "Demonstration of a 1.1 petawatt laser based on a hybrid optical parametric chirped pulse amplification/mixed Nd:glass amplifier," Appl. Opt. **49**, 1676 (2010).
6. J. H. Sung, S. K. Lee, T. J. Yu, T. M. Jeong, and J. Lee, "0.1 Hz 1.0 Pw Ti:sapphire laser," Opt. Lett. **35**, 3021 (2010).
7. C. Liu, S. Banerjee, J. Zhang, S. Chen, K. Brown, J. Mills, N. Powers, B. Zhao, G. Golovin, I. Ghebregziabher, and D. Umstadter, "Repetitive petawatt-class laser with near-diffraction-limited focal spot and transform-limited pulse duration," Proc. SPIE **8599**, 859919 (2013).
8. J. H. Sung, H. W. Lee, J. Y. Yoo, J. W. Yoon, C. W. Lee, J. M. Yang, Y. J. Son, Y. H. Jang, S. K. Lee, and C. H. Nam, "4.2 PW, 20 fs Ti:sapphire laser at 0.1 Hz," Opt. Lett. **42**, 2058 (2017).
9. Z. Gan, L. Yu, S. Li, C. Wang, X. Liang, Y. Liu, W. Li, Z. Guo, Z. Fan, X. Yuan, L. Xu, Z. Liu, Y. Xu, J. Lu, H. Lu, D. Yin, Y. Leng, R. Li, and Z. Xu, "200 J high efficiency Ti:sapphire chirped pulse amplifier pumped by temporal dual-pulse," Opt. Express **25**, 5169 (2017).
10. H. T. Kim, I. J. Kim, C. M. Kim, T. M. Jeong, T. J. Yu, S. K. Lee, J. H. Sung, J. W. Yoon, H. Yun, S. C. Jeon, I. W. Choi, and J. Lee, "Single-shot nanometer-scale holographic imaging with laser-driven x-ray laser," Appl. Phys. Lett. **98**, 121105 (2011).
11. I. J. Kim, K. H. Pae, I. W. Choi, C.-L. Lee, H. T. Kim, H. Singhal, J. H. Sung, S. K. Lee, H. W. Lee, P. V. Nickles, T. M. Jeong, C. M. Kim, and C. H. Nam, "Radiation pressure acceleration of protons to 93 MeV with circularly polarized petawatt laser pulses," Phys. Plasmas **23**, 070701 (2016).

Optics EXPRESS

12. H. T. Kim, V. B. Pathak, K. H. Pae, A. Lifschitz, F. Sylla, J. H. Shin, C. Hojbota, S. K. Lee, J. H. Sung, H. W. Lee, E. Guillaume, C. Thaury, K. Nakajima, J. Vieira, L. O. Silva, V. Malka, and C. H. Nam, "Stable multi-GeV electron accelerator driven by waveform-controlled PW laser pulses," Sci. Reports **7**, 10203 (2017).
13. T. Heinzl, "Compton scattering at high intensities," J. Physics: Conf. Ser. **198**, 012005 (2009).
14. A. Di Piazza, C. Müller, K. Z. Hatsagortsyan, and C. H. Keitel, "Extremely high-intensity laser interactions with fundamental quantum systems," Rev. Mod. Phys. **84**, 1177 (2012).
15. S. Ataman, M. Cuciuc, L. D'Alessi, L. Neagu, M. Rosu, K. Seto, O. Tesileanu, Y. Xu, and M. Zeng, "Experiments with combined laser and gamma beams at ELI-NP," AIP Conf. Proc. **1852**, 070002 (2017).
16. S. Gales, K. A. Tanaka, D. L. Balabanski, F. Negoita, D. Stutman, O. Tesileanu, C. A. Ur, D. Ursescu, I. Andrei, S. Ataman, M. O. Cernaianu, L. D'Alessi, I. Dancus, B. Diaconescu, N. Djourelov, D. Filipescu, P. Ghenuche, D. G. Ghita, C. Matei, K. Seto, M. Zeng, and N. V. Zamfir, "The extreme light infrastructure—nuclear physics (ELI-NP) facility: new horizons in physics with 10 PW ultra-intense lasers and 20 MeV brilliant gamma beams," Rep. Prog. Phys. **81**, 094301 (2018).
17. J. D. Zuegel, S.-W. Bahk, I. A. Begishev, J. Bromage, C. Dorrer, A. V. Okishev, and J. B. Oliver, "Status of high-energy OPCPA at LLE and future prospects," in *CLEO: 2014,* (Optical Society of America, 2014), p. JTh4L.4.
18. J. Zou, C. Le Blanc, D. Papadopoulos, G. Chériaux, P. Georges, G. Mennerat, F. Druon, L. Lecherbourg, A. Pellegrina, P. Ramirez, F. Giambruno, A. Fréneaux, F. Leconte, D. Badarau, J. Boudenne, D. Fournet, T. Valloton, J. Paillard, J. Veray, M. Pina, P. Monot, J. Chambaret, P. Martin, F. Mathieu, P. Audebert, and F. Amiranoff, "Design and current progress of the Apollon 10 PW project," High Power Laser Sci. Eng. **3**, e2 (2015).
19. L. Xu, L. Yu, X. Liang, Y. Chu, Z. Hu, L. Ma, Y. Xu, C. Wang, X. Lu, H. Lu, Y. Yue, Y. Zhao, F. Fan, H. Tu, Y. Leng, R. Li, and Z. Xu, "High-energy noncollinear optical parametric-chirped pulse amplification in LBO at 800 nm," Opt. Lett. **38**, 4837 (2013).
20. F. Druon, G. Chériaux, J. Faure, J. Nees, M. Nantel, A. Maksimchuk, G. Mourou, J. C. Chanteloup, and G. Vdovin, "Wave-front correction of femtosecond terawatt lasers by deformable mirrors," Opt. Lett. **23**, 1043 (1998).
21. T. M. Jeong, I. W. Choi, N. Hafz, J. H. Sung, S. K. Lee, D.-K. Ko, and J. Lee, "Wavefront correction and customization of focal spot of 100 TW Ti:sapphire laser system," Jpn. J. Appl. Phys. **46**, 7724 (2007).
22. S. Fourmaux, S. Payeur, A. Alexandrov, C. Serbanescu, F. Martin, T. Ozaki, A. Kudryashov, and J. C. Kieffer, "Laser beam wavefront correction for ultra high intensities with the 200 TW laser system at the advanced laser light source," Opt. Express **16**, 11987 (2008).
23. S.-W. Bahk, P. Rousseau, T. A. Planchon, V. Chvykov, G. Kalintchenko, A. Maksimchuk, G. A. Mourou, and V. Yanovsky, "Generation and characterization of the highest laser intensities (10^{22} W/cm^2)," Opt. Lett. **29**, 2837 (2004).
24. V. Yanovsky, V. Chvykov, G. Kalinchenko, P. Rousseau, T. Planchon, T. Matsuoka, A. Maksimchuk, J. Nees, G. Cheriaux, G. Mourou, and K. Krushelnick, "Ultra-high intensity-300-TW laser at 0.1 Hz repetition rate," Opt. Express **16**, 2109 (2008).
25. A. S. Pirozhkov, Y. Fukuda, M. Nishiuchi, H. Kiriyama, A. Sagisaka, K. Ogura, M. Mori, M. Kishimoto, H. Sakaki, N. P. Dover, K. Kondo, N. Nakanii, K. Huang, M. Kanasaki, K. Kondo, and M. Kando, "Approaching the diffraction-limited, bandwidth-limited petawatt," Opt. Express **25**, 20486 (2017).
26. Z. Guo, L. Yu, J. Wang, C. Wang, Y. Liu, Z. Gan, W. Li, Y. Leng, X. Liang, and R. Li, "Improvement of the focusing ability by double deformable mirrors for 10-PW-level Ti: sapphire chirped pulse amplification laser system," Opt. Express **26**, 26776 (2018).
27. J.-C. F. Chanteloup and M. Cohen, "Compact high resolution four wave lateral shearing interferometer," Proc. SPIE **5252**, 282 (2004).
28. S. Kahaly, S. Monchocé, V. Gallet, O. Gobert, F. Réau, O. Tcherbakoff, P. D'Oliveira, P. Martin, and F. Quéré, "Investigation of amplitude spatio-temporal couplings at the focus of a 100 TW-25 fs laser," Appl. Phys. Lett. **104**, 054103 (2014).
29. V. Bagnoud, "Amplification of high-fidelity laser pulses," Habilitation, Technische Universität Darmstadt (2016).
30. K. Nakamura, H. Mao, A. J. Gonsalves, H. Vincenti, D. E. Mittelberger, J. Daniels, A. Magana, C. Toth, and W. P. Leemans, "Diagnostics, control and performance parameters for the bella high repetition rate petawatt class laser," IEEE J. Quantum Electron. **53**, 1–21 (2017).